

An Investigation of 19.5 GHz Sky Noise Temperature over Taiwan Area

Yen-Hsyang Chu¹ and Shun-Peng Shih¹

(Manuscript received 28 September 1999, in final form 10 November 1999)

ABSTRACT

A number of ground-based instruments, including 19.5 GHz radiometer, optical raingauge, portable weather station, and high resolution disdrometer, were set up to conduct the Ka band propagation experiment of the Experimental Communication Payload (ECP) for ROCSAT-1. In this article, 19.5 GHz background sky noise temperatures measured at Chung-Li and Tainan sites are presented and investigated. Long-term statistics of the 19.5 GHz background sky noise temperature observed by a vertically pointed radiometer in precipitation-free condition over the Taiwan area shows that the percentages of time that the sky noise temperature exceeds 20 K, 30 K, 40 K and 50 K are, respectively, 98%, 85%, 53%, and 27%. However, in precipitating environments, statistics shows that the percentage of time that the sky noise temperature exceeds 55 K, 100 K, 150 K, and 200 K are, respectively, 22%, 13%, 4.5%, and 2%. The statistics of sky noise temperatures observed at different zenith angles under environments without precipitation is also made. The results show that 80% of the observed sky noise temperatures at zenith angles of 10°, 30°, 50° and 70° are, respectively, in the ranges of 92 – 180 K, 39 – 52 K, 26 – 33 K, and 21 – 27 K. In addition, a comparison between surface rainfall rate recorded by the optical raingauge and sky noise temperature measured by 19.5 GHz radiometer shows that the former lags behind the latter by about 5 minutes, implying non-uniform and inhomogeneous distribution of precipitation in the air. In order to measure the precipitation aloft, the Chung-Li VHF radar was operated simultaneously. Champaign observation shows that there is no latency between sky noise temperature and VHF backscatter from precipitation. This result implies that the VHF backscatter from precipitation can be employed to validate the observed sky noise temperature. In addition, we also find that the sky noise temperature may be as high as 155 K (corresponding to 3.6 dB attenuation) under an environment without surface precipitation. This feature is attributed to the dense water vapor and heavy cloud.

(Key words: Radiometer, VHF radar, Ka band, Precipitation)

¹Institute of Space Science, National Central University, Chung-Li, Taiwan, ROC

1. INTRODUCTION

The first scientific experimental satellite, ROCSAT-1, was successfully launched on January 27, 1999. This one is a low-earth orbit (LEO) satellite orbiting at altitude of about 600 km with an inclination of 35° and an orbital period of 97 minutes. The frequencies of uplink and downlink signals of the ROCSAT-1 for TT&C (Telemetry, Tracking and Command), located at Chung-Li and Tai-nan, are 2039.6 and 2215 MHz, respectively. The total weight (with payloads and fuel) of ROCSAT-1 is 395 kg and the mission life in orbit is at least 2 years. There are three payloads mounted on the ROCSAT-1. The first one is the Ocean Color Imager (OCI) for remote sensing of the pigment distribution in the low-latitude oceans for the oceanography research. The second payload is the Ionospheric Plasma and Electrodynamics Instrument (IPEI) used for taking measurements of ionospheric parameters, including plasma density, plasma temperature, electric field strength, plasma drift velocity, and so on. The third payload is the Experimental Communication Payload (ECP) designed for communication experiments, including the Ka band propagation experiment. In order to conduct the propagation experiment, besides the 19.5 GHz beacon transmitter on board, a number of ground-based instruments were set up. For example, three optical raingauges were installed in Chung-Li, Hsin-Chu, and Tai-nan respectively to record the surface rainfall rates with high temporal resolution (less than one minute). The algorithm of signal processing and analysis for the Chung-Li VHF radar returns was developed to obtain the information about precipitation aloft. A 19.5 GHz radiometer in combination with a set of portable weather station was employed to measure the background sky noise temperature. For more information on the characteristics of these ground-based instruments, see Shih and Chu (1999a).

It is generally recognized that electromagnetic waves at the Ka band are susceptible to weather-related precipitation, impairing the quality of the Earth-satellite communication (Hogg and Chu, 1975). Except for the rain attenuation through the absorption and scattering effects, the absorption by oxygen molecules and water vapor, scattering and diffraction by the atmospheric refractivity irregularities, and abnormal refracting by the stratification of atmospheric structures play the most important roles in the degradation of the earth-satellite communication link. In order to design an optimal earth-satellite communication link over Taiwan area, the environmental effects influencing the quality of satellite communication mentioned above should be investigated thoroughly. The plausible objectives of the Ka band propagation experiment in ECP are to study the characteristics of rain attenuation, behavior of scintillation caused by refractivity fluctuations, depolarization effect on Ka band signal due to non-spherical rain drop, development of the techniques of overcoming rain attenuation, multi-path and low-elevation propagation effects.

With employment of the ground-based radiometer mentioned above, the long-term statistics of 19.5 GHz background sky noise temperature measured at the Chung-Li and Tai-nan sites are presented and discussed in this article. According to the authors' knowledge, the characteristics of the 19.5 GHz sky noise temperature over the Taiwan area has not been previously investigated and reported. Basically, the sky noise temperature results from the background emissions, either from atmospheric constituents (water vapor and oxygen molecules) or hydrometeor particles. The intensity of the sky noise temperature is proportional to the

densities of water vapor, oxygen molecules, and hydrometeor particles. As a result, the observation of sky noise temperature can be employed to estimate the water vapor concentration and rainfall rate. However, before doing so, a great caution should be taken in processing the observed data. For example, we will show in this article that a significant time delay between sky noise temperature and surface rainfall rate is seen. Therefore, inaccurate results will be produced if the time delay is not corrected and the data are not adjusted. Furthermore, one-to-one correspondence of surface rainfall rate to sky noise temperature may not be achieved because the hydrometeor particles existing in the air may not fall to the ground due to the effects of evaporation and drift with the background wind. In this case, with the help of capability of measuring hydrometeor particles aloft, the Chung-Li VHF radar can be used to identify the occurrence of the precipitation aloft. A campaign observation of precipitation made with Chung-Li VHF radar, 19.5 GHz radiometer, and high resolution optical raingauge was carried out and the results are presented and discussed below in this article.

This paper is organized as follows: The long-term statistics of background 19.5 GHz sky noise temperatures observed at Chung-Li and Tai-Nan sites in the precipitation-free environment are presented and discussed in Section 2. The comparison between surface rainfall rate, 19.5 GHz sky noise temperature, and VHF backscatter from precipitation are shown and discussed in Section 3. And ,the conclusion is presented in Section 4.

2. LONG-TERM STATISTICS OF 19.5 GHZ SKY NOISE TEMPERATURE

The sky noise temperature observed by a 19.5 GHz radiometer consists primarily of the radiations from water vapor, oxygen molecules, and hydrometeors, in which the precipitation particles (especially liquid rain drop) contribute to most of the observed sky noise temperature in the precipitating environment. The cosmic and galactic radiations are usually neglected in the investigation of sky noise temperature because of their enormously weak intensities (2.7 K for the former and less than 1 K for the latter at 19.5 GHz) (Ulaby et al., 1981). In a precipitation-free environment, the intensity of 19.5 GHz sky noise temperature is governed by the concentration of water vapor. Calculations show that the specific attenuations of oxygen molecule and water vapor at 19.5 GHz under the condition of pressure 1013 mb and temperature 20°C is, respectively, about 0.01 and 0.07 dB/km, provided the concentration of water vapor is 7.5 g/m³ (corresponding to relative humidity of about 43%). Therefore, the observation of 19.5 GHz sky noise temperature can be employed to investigate the behavior of water vapor and precipitation.

The data employed for the long-term statistical analysis in this article are the 19.5 GHz sky noise temperature recorded by a vertically pointed radiometer located at Chung-Li and Tai-Nan from February 13, 1998, to September 21, 1999. The integration time of radiometer is 0.5 s and the sampling interval of the data for statistics is 10 s. For detailed information on the characteristics of the radiometer, see Shih and Chu (1999a). Figure 1 presents the cumulative distribution of the 19.5 GHz sky noise temperature, where the percentage of time in the period that the sky noise temperature exceeds a certain value is marked on the ordinate. Note that the parameters shown in the bottom and upper abscissa are different. The former is the sky noise

temperature and the latter is the corresponding attenuation. The mathematical relation converting the observed sky noise temperature T_b into the attenuation can be expressed as follows

$$A = 10\log_{10}(T_a/(T_a-T_b)) \quad (1)$$

where A is the attenuation in unit of dB, T_b is the observed sky temperature in unit of K, T_a is the apparent temperature of absorber and the value of 275 K is used in converting T_b into A in this study, as suggested by Hogg and Chu (1975). As indicated from Fig. 1, the distribution of the sky noise temperature consists of two parts. One part of the distribution has a sharp roll-off rate in the interval of 10 – 50 K, while the other part of the distribution has a smoother slope in the region of 50 – 275 K. Examining the weather conditions under which the radiometry experiments were carried out indicates that the former corresponds to the sky noise temperature observed in clear-air and cloudy conditions, while the latter is for a precipitation environment. Statistics shows that in a precipitation-free environment 80% of the observed sky noise temperature over Taiwan area is within 23 - 48 K and 90% of the sky noise temperature will be greater than 30 K (corresponding to attenuation of about 0.5 dB). The minimum and maxi-

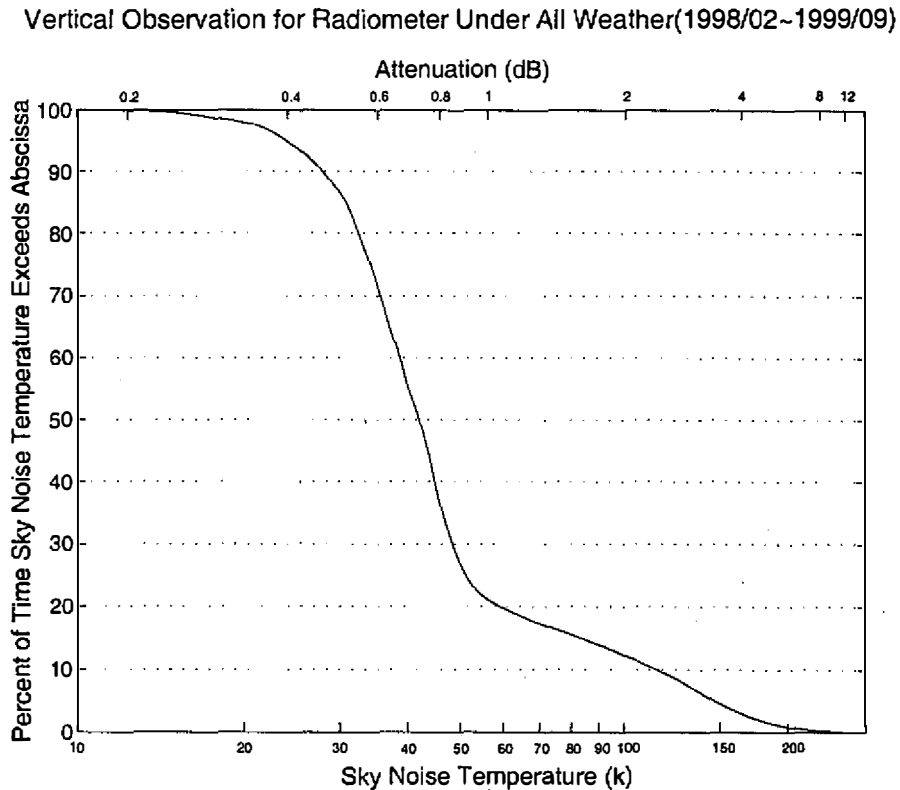


Fig. 1. Long-term statistics of sky noise temperature at 19.5 GHz over Taiwan area.

imum sky noise temperatures are, respectively, 13 K and 55 K. However, for the condition of precipitation, the range of sky noise temperature is between 55 K and 250 K, depending on the intensity of rainfall rate. A case study of the comparison between sky noise temperature and surface rainfall rate recorded by an optical raingauge will be presented and discussed later. An interesting feature presented in Fig. 1 is the crossover of curves for clear-air and precipitation sky noise temperatures. As indicated, the crossover occurs at 55 K, corresponding to the attenuation of about 1 dB. This implies that the maximum attenuation of 19.5 GHz EM wave propagation in the precipitation-free environment will be about 1 dB over Taiwan area. In addition, Fig. 1 also demonstrates that the percentage of time that the precipitation occurs in the observation period is less than 20%.

In addition to the vertical observations, the experiments of sky noise temperature measurement at different elevation angles were also conducted using the 19.5 GHz radiometer. Figure 2 shows the variations of sky noise temperature with elevation angle in the step of 10° under the clear-air and partly cloudy conditions, where the curves in the plot represent the cumulative probability of the sky noise temperature that exceeds abscissa. It is obvious from Fig. 2 that the sky noise temperature is highly elevation angle-dependent. The probability that the sky noise temperature at 10° elevation angle is greater than 150 K (corresponding to propagation attenuation of about 3.5 dB) is 50%. In addition, for the curve marked with 75% cumulative probability, the sky noise temperature changes from 150 K at 10° to 39 K at 70° . The feature of high sky noise temperature is attributed to the large concentration of water vapor over Taiwan area. This large attenuation will impair the tracking of satellites at low elevation angles. In view of large variation in rain attenuation with elevation angle, the propagation margin should be large enough to achieve high link reliability in designing the communication link for a LEO satellite. A new method of estimating the precipitable water vapor content in clear-air condition using the variation of sky noise temperature with elevation angle observed by single ground-based radiometer has been developed by Shih and Chu (1999b). By this method, a theoretical model connecting atmospheric propagation loss and absorption (or attenuation) of EM wave due to water vapor and oxygen molecule is developed to best fit to observed data in accordance with a non-linear least-squares method. A comparison of precipitable water vapor contents estimated from radiometer data and obtained by rawinsonde is also made. The result shows a good agreement between them, indicating the validity of this method. Therefore, the information contained in Fig. 2 can be employed not only for the design of a Ka band communication system for earth-satellite link, but also for the estimation of precipitable water vapor content.

3. CAMPAIGN OBSERVATIONS OF PRECIPITATION

It is well-known that a heavy rainfall rate will result in enormously large sky noise temperature and cause severe attenuation of EM wave at Ka band due to absorption of precipitation particles. Therefore, employing the radiometer at Ka band in combination with the proper raingauge to record high resolution rainfall rate, the precipitation can be observed and investigated accordingly. However, the information of height variation of precipitation aloft cannot

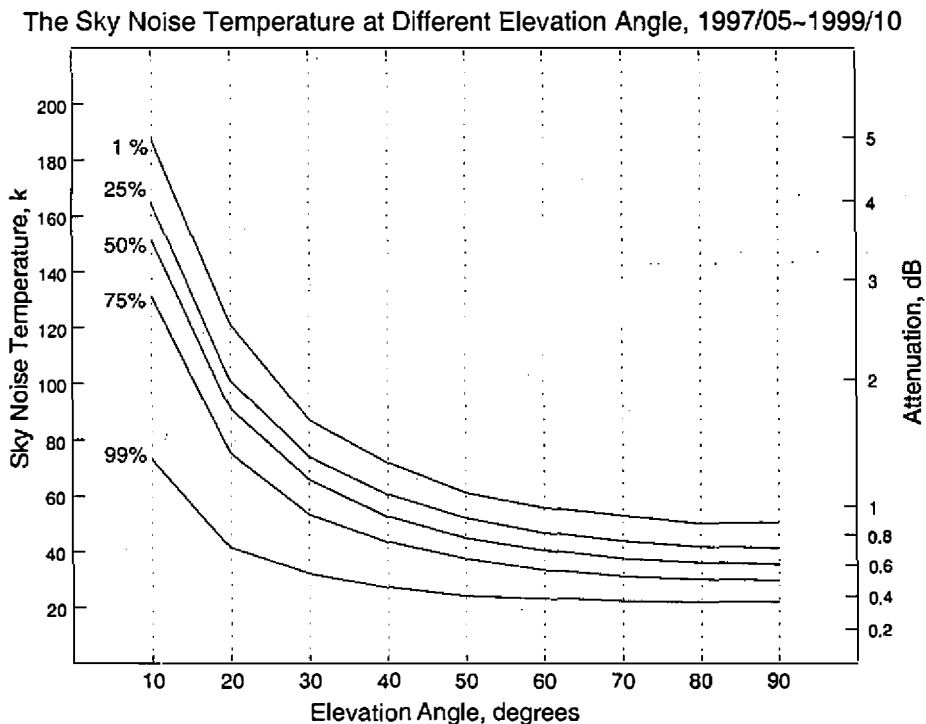


Fig. 2. Statistics of variation of sky noise temperature with elevation angle in the precipitation-free environment

be obtained from the measurements of a single radiometer and ground-based raingauge, leading to the blind zone of the collection of precipitation data. In order to overcome this difficulty, the Chung-Li VHF radar is employed for the campaign measurement of the precipitation in the air. The capability of a VHF radar to observe precipitation and clear-air turbulent activity simultaneously has been recognized by scientific community for many years. With this capability, many precipitation-related parameters and features that cannot be obtained directly from a single conventional microwave meteorological radar, including terminal velocity of hydrometeor, drop-size distribution, 3-dimensional wind field in a raincloud, severe depletion of clear-air VHF echo power associated with precipitation, frozen-in property of hydrometeor, can be observed by using a VHF radar (Wakasugi et al., 1986; Chu et al., 1991; Chu et al., 1994; Chu et al., 1997; Chu et al., 1998). Therefore, the use of radiometer in combination with VHF radar and surface raingauge will be a great benefit in the investigation of precipitation.

Figure 3 shows a typical example of the contour plot of observed Doppler power spectra varied with height in the precipitation environment made by the Chung-Li VHF radar. The radar parameters were set as follows. Pulse length was $2 \mu\text{s}$ (corresponding to 300 m range resolution), inter-pulse period was $500 \mu\text{s}$, coherent integration time was 0.03 s, 40 range gates were set, and three radar beams were pointed vertically. As shown in Fig. 3, there are two salient spectral components occurred simultaneously in the plot. One of the spectral components with intense echo power located at around zero Doppler velocity are the echoes from

refractivity fluctuations. However, the other spectral components with downward (or negative) Doppler velocity correspond to the echoes from precipitation. A large change in the Doppler velocity for the precipitation spectral component in the height range 5.1 – 4.8 km, where the echo powers are strengthened significantly, is thought to be due to the bright band (or melting layer) effect. Obviously, it is easy to separate the precipitation echoes from refractivity fluctuation echoes in the Doppler spectrum, making extractions of information about precipitation and turbulence from the Doppler spectrum of VHF radar possible. Once the differentiation of precipitation echoes from turbulence echoes in the observed Doppler spectrum is completed, the echo powers and the mean Doppler velocities of the precipitation and refractivity fluctuations can be obtained by computing the zero and first moment of the spectrum using the moment method. Figs.4a and 4b present the height-time-intensity plots for turbulence and precipitation, respectively. It is noteworthy that the echo power of refractivity fluctuations as a function of potential temperature, specific humidity and pressure is proportional to the gradient of generalized potential refractive index M defined as follows (Ottersten, 1969; Tatarskii, 1971; Chu et al., 1990)

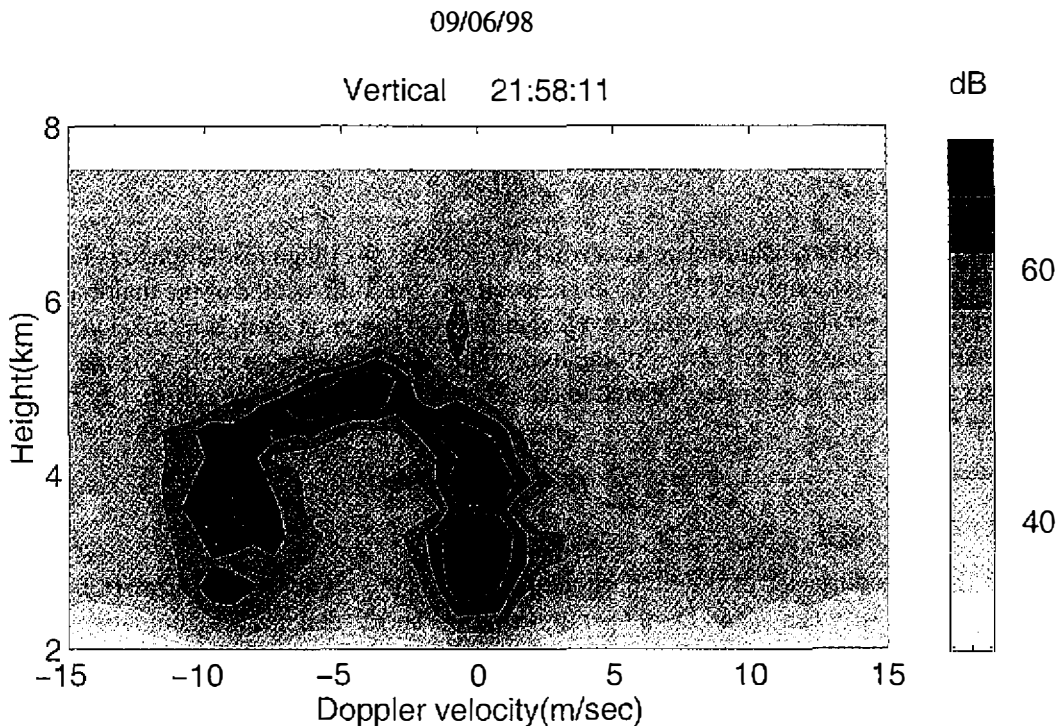


Fig. 3. Example of height variation of Doppler power spectra observed by using a vertically pointed radar beam of Chung-Li VHF radar, where the spectral component located at around zero Doppler frequency velocity is the echoes from refractivity fluctuations and that with Doppler frequency velocity of about -9 m/s is precipitation echoes.

$$M = -77.6 \times 10^{-6} \frac{P}{T} \frac{\partial \ln}{\partial z} \left[1 + \frac{15,500q}{T} \left(1 - \frac{1}{2} \frac{\partial \ln q / \partial z}{\partial \ln \theta / \partial z} \right) \right] \quad (2)$$

where T is temperature (K), P is pressure (mb), q is the specific humidity which is essentially the same as mixing ratio w , and θ is potential temperature (K). It has been shown by many investigators that the VHF radar echo intensity arising from refractivity fluctuations correlates very well with the square of M (Tsuda et al., 1988; Chu et al., 1990). This behavior indicates that the decrease of the water vapor content will reduce the magnitude of M and, hence, lower the VHF radar reflectivity from turbulent air. In light of the fact that the magnitude of M is dominated by the specific humidity and its gradient, the turbulent echo power will be governed by the humidity.

As for the echoes from precipitation, the echoing mechanism can be treated as Rayleigh scattering because the wavelength of the Chung-Li VHF radar (about 5.77 m) is considerably greater than the diameter of hydrometeors (less than a few millimeter). The corresponding radar equation can be described as follows (Rogers, 1979)

$$P_s = \frac{\pi^4 P_t \theta \phi G A_e |K|^2 Z}{128 \ln 2 \lambda^4 Z^2} \Delta R = C \frac{|K|^2 Z}{Z^2} \Delta R \quad (3)$$

where P_t is the peak transmitted power (W), $\Delta R (=c\tau/2)$ is the range resolution, c is light speed (m/s), τ is the pulse length (s), θ and ϕ are respectively the 3-dB widths of the major and minor axes of the antenna beam, λ is radar wavelength (m), G is antenna gain, $K = (m^2 - 1)/(m^2 + 1)$, m is the complex index of refraction of the hydrometeor, z is the range (m), A_e is the effective antenna aperture, C is a constant related to radar parameters, and Z is the reflectivity factor and defined by

$$Z = \sum_v D_i^6 = \int N(D) D^6 dD \quad (4)$$

where D_i is the diameter of the i th particle, $N(D)dD$ is the number of precipitation particles with diameters between D and $D+dD$ per unit volume, and \sum_v denotes the summation over unit volume. Note that the mean Doppler terminal velocity V_t of precipitation particle is defined by

$$V_t = \frac{\int V(D) N(D) D^6 dD}{\int N(D) D^6 dD} \quad (5)$$

where $V(D)$ is the hydrometeor fall speed with respect to still air. As indicated in Fig. 4b, the precipitation occurs intermittently in the height range under 6 km over the period from about

21:20 LT to 22:17 LT. An interesting feature shown in Fig. 4b is the enhancement of precipitation echo power in the height range 5.2 – 4.5 km, called bright band structure. This feature is strongly related to the behavior of the melting layer, including height, thickness, temperature distribution, vertical air velocity, and so on. According to the temperature sounding made by Pan-Chiao rawinsonde station (located from the Chung-Li VHF radar about 25 km northeast), the height of 0°C isotherm locates at about 5.2 km, consistent with the radar observation of the bright band.

Figure 5 presents the surface rainfall rate recorded by the optical raingauge situated on the campus of National Central University. It is clear from Fig. 5 that the surface rain with maximum rainfall rate of about 4 mm/hr is recorded intermittently, and its occurrence coincides with the measurement of VHF radar. A comparison of rainfall measurements made by surface raingauge and VHF radar shows that a one-to-one correspondence between the precipitation records made by VHF radar and surface optical raingauge is seen. However, examining Fig. 4b and 5 in more detail reveals that the precipitation aloft may not necessarily agree with the rainfall rate recorded on the ground, as shown in the period 22:06 LT – 22:15 LT in the Figs. 4a and 5. This feature suggests that the attenuation of the Ka band signal propagation in the air can be abnormally high even in the condition of no rainfall on the surface. In addition, comparing Figs. 4b and 5 in more detail indicates that there is a remarkable time difference between these two records. Cross-correlation analysis further shows that on average the precipitation recorded by surface optical raingauge lags the precipitation aloft observed by the VHF radar by about 5 minutes. This feature was also observed and reported by Chu and Song (1998). However, the time lag reported by the latter (about 7 – 13 minutes) is much greater than in the present case. We believe that the difference of time lag between the two presumably can be attributed to the different vertical air velocities affecting the falling speed of hydrometeors. This shows that the vertical air velocity for the case studied by Chu and Song (1998) is generally upward and within the range 0.2 – 1.5 m/s. However, the vertical air velocities observed in this case are basically downward and have the magnitude in the range –1.5 – 2.0 m/s, as shown in Fig. 6. The behavior of intermittent precipitation and the time difference between the precipitations that occurred in the air and that were recorded on the ground suggests that the distribution of the intensity of the precipitation for this event is not uniform in the height range in which the precipitation occurs.

Figure 7 presents the sky noise temperature observed by the upward-looking 19.5 GHz radiometer over the same interval as the experiments of VHF radar and optical raingauge, where the locations of VHF radar, optical raingauge and radiometer of precipitation are all on the campus of National Central University for the campaign observation. A comparison of Fig. 6 and Fig. 7 shows that basically the precipitation events on the ground presented in Fig. 6 correspond to the enhancement of sky noise temperature. Cross correlation analysis of the data between radiometer and optical raingauge shows a time difference in the two, where the latter lags the former by about 4.6 minutes. This time difference is quite consistent with that between radar data and optical raingauge data as mentioned above. Inspecting Fig. 7 in more detail demonstrates that the sky noise temperature is still high even after the precipitations are over. It is noteworthy that the magnitude of background sky noise temperature in the precipitation-free environment is generally in the range 10 – 50 K, as shown in Fig. 1. However, Fig.

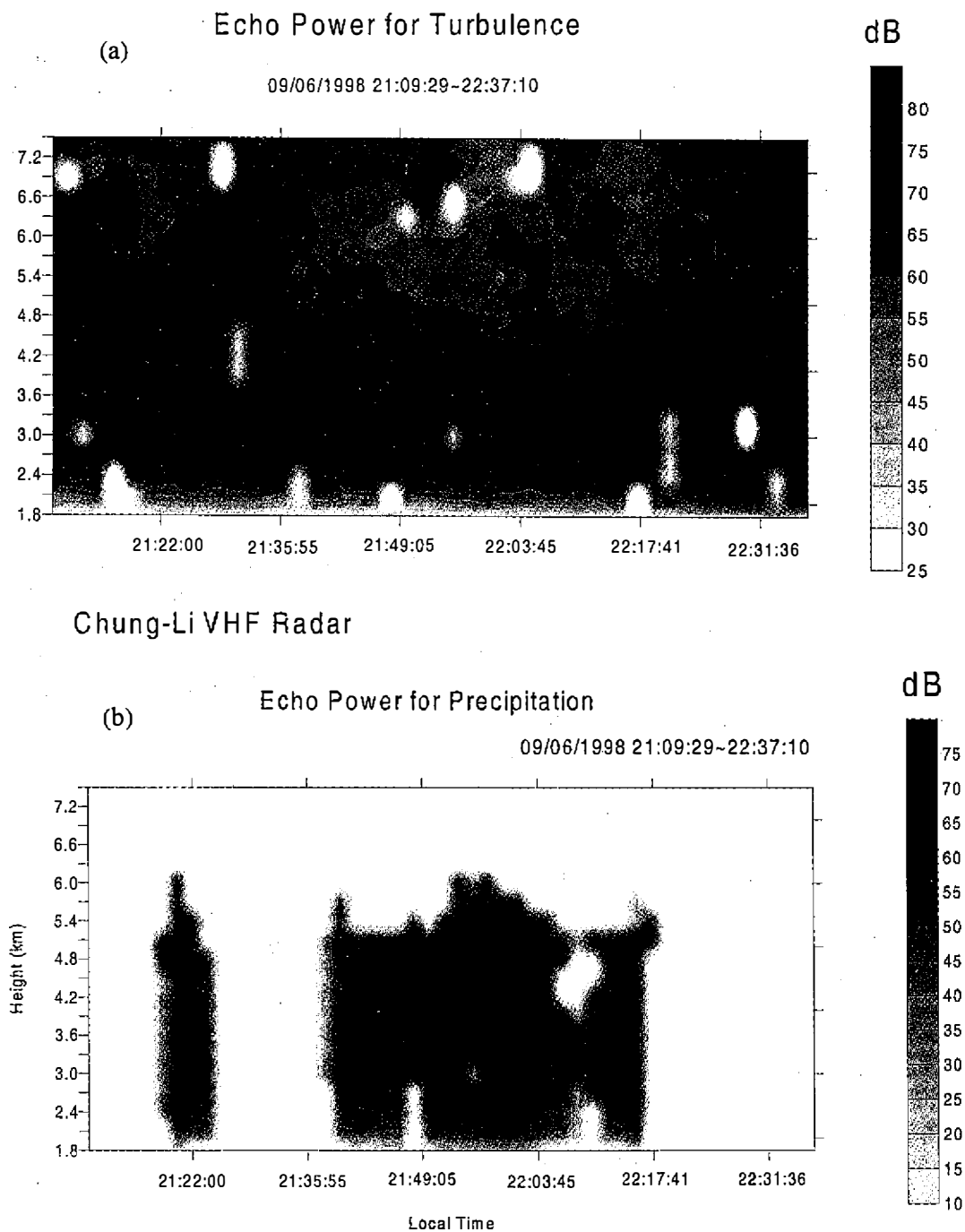


Fig. 4. (a) Height-time-intensity plot for the VHF radar echoes from atmospheric refractivity fluctuations. (b) Height-time-intensity plot for the VHF radar echoes from precipitation.

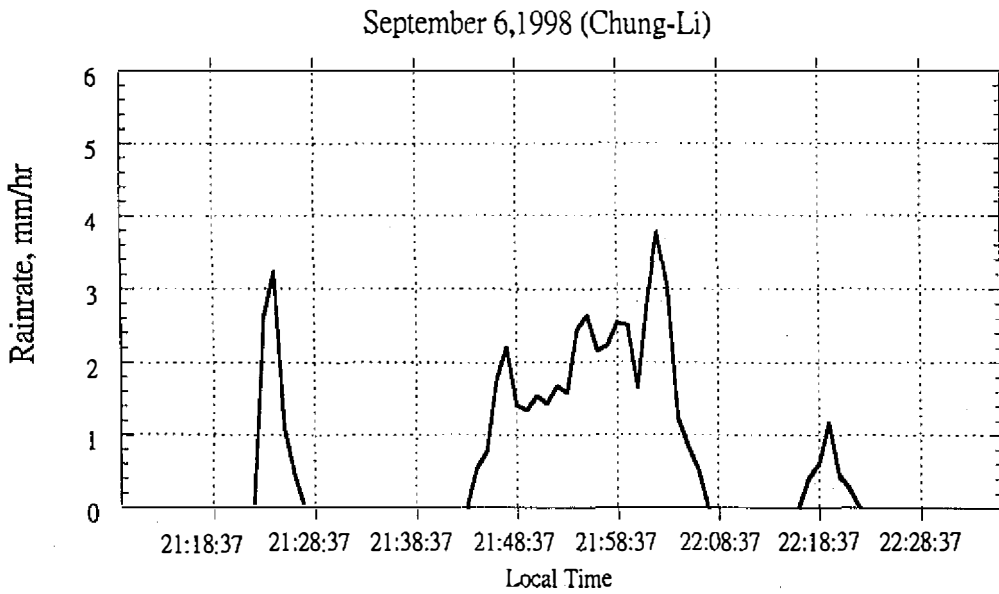


Fig. 5. Surface rainfall rate observed by optical raingauge located on the campus of National Central University.

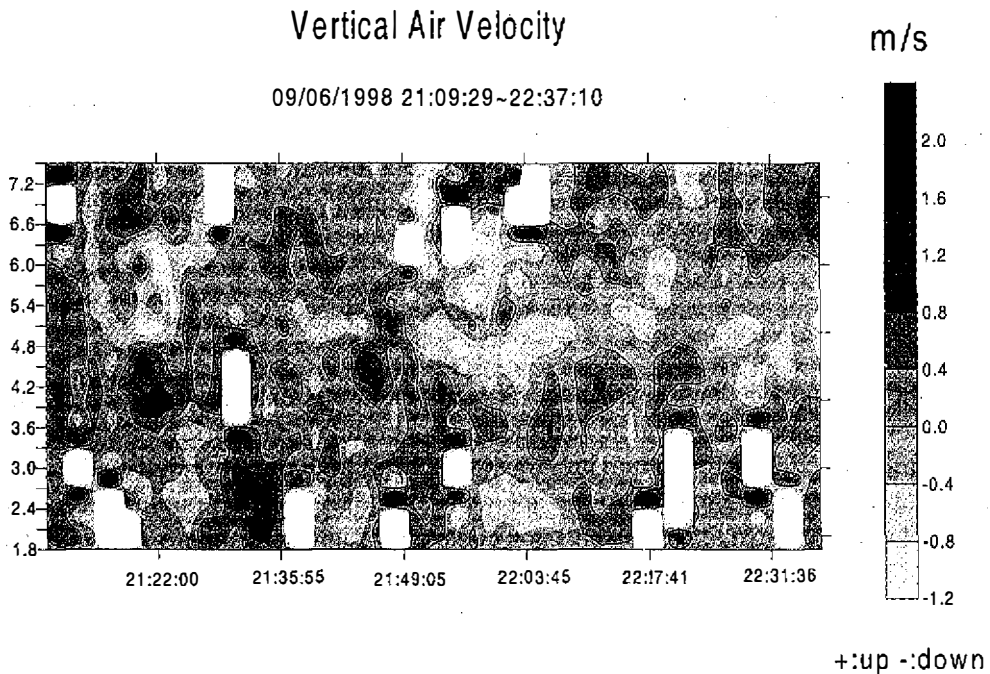


Fig. 6. Height-time-magnitude of vertical air velocity estimated from the turbulent spectral component of observed Doppler power spectra using the moment method.

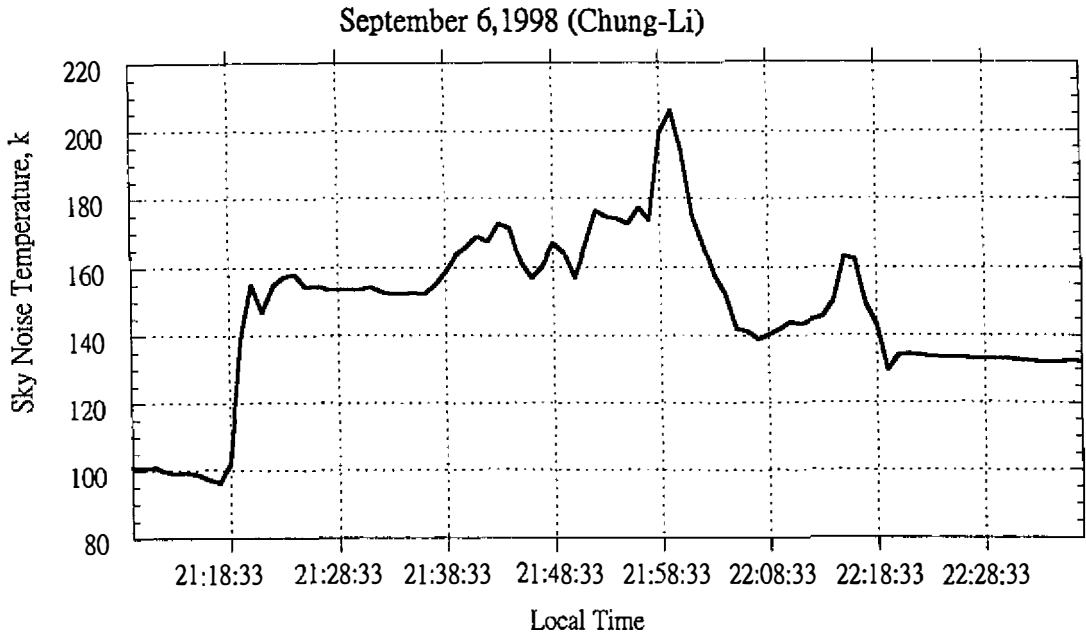


Fig. 7. Sky noise temperature measured by 19.5 GHz radiometer located on the campus of National Central University.

7 indicates that the sky noise temperature recorded in the period of no surface rainfall can be as large as 155 K. It is well known that sky noise temperature increases with the increase of the surface rainfall rate (Hogg, 1989). An empirical relationship between sky noise temperature T_b observed by a 19.5 GHz radiometer and surface rainfall rate R has been established by Shih and Chu (1999a) as follows:

$$T_b = 102.4 + 8.044R \quad (6)$$

where the assumption that the apparent rain temperature is 275 K is made. With the help of equation (6), it is easy to calculate that the apparent rainfall rate corresponding to 155 K sky noise temperature is about 6.6 mm/hr, larger than the rainfall rate observed on the ground. The corresponding rain attenuation to the apparent rainfall rate of 6.6 mm/hr can be estimated below. It is well known that the expression connecting rain attenuation A and rainfall rate R is

$$A = aR^bL \text{ (in dB)} \quad (7)$$

where L is the path length of the EM wave propagation and the values of a and b at 19.5 GHz are, respectively, 0.07 and 1.12 (Ippolito, 1986). From the precipitation observations made by the Chung-Li VHF radar as shown in Fig. 4b, the value of path length L can be taken to be 5 km, which is the height of rain in the air. Therefore, computation shows that the corresponding

rain attenuation to apparent rainfall rate of 6.6 mm/hr is about 3 dB, quite consistent with the result obtained using the inversion of sky noise temperature to the attenuation in accordance with equation (1). It is generally believed that the intense water vapor and dense cloud particles contributing significantly to the background sky noise temperature is a common feature over Taiwan area, especially for Ka band signal. As a result, an abnormal absorption of the Ka band satellite signal is generated and hence an extra attenuation of the signal will be expected, impairing further the earth-satellite communication at the Ka band. Therefore, more investigations on this issue are needed to understand the effects of dense cloud and heavy water vapor content on the earth-satellite communication system at Ka band.

4. CONCLUDING REMARKS

The long-term statistical analysis of the 19.5 GHz sky noise temperature observed by an upward-looking radiometer located at Chung-Li and Tai-nan from February 13, 1998, to September 21, 1999 is presented in this article. It shows that the background sky noise temperature in precipitation-free conditions has values in the range of 10 – 50 K, while 50 – 275 K for precipitation environment. In addition to the vertical observation, the statistics of the variation of sky noise temperature with elevation angle is also made in this article. It shows that more than 75% of the sky noise temperatures at the elevation angles 10°, 20°, 30°, 40°, 50°, 60°, 70°, and 80° exceed 130 K, 78 K, 56 K, 43 K, 39 K, 36 K, 34 K, and 32 K, respectively. A campaign experiment of precipitation, including 19.5 GHz radiometer, high resolution optical raingauge, and Chung-Li VHF radar, was conducted to investigate the behavior of precipitation in the air. We found that a remarkable time difference between the data recorded by surface raingauge and radiometer is seen, in which the former lags behind the latter by about 5 minutes. A similar time difference can also be seen between the data observed by optical raingauge and VHF radar. A comparison between sky noise temperature and surface rainfall rate shows that, in a certain period where no surface rainfall rate is measured, the observed 19.5 GHz sky noise temperature may still be high, even over 155 K. On the basis of an empirical expression connecting surface rainfall rate and 19.5 GHz sky noise temperature, it is easy to show that this high sky noise temperature is equivalent to the apparent surface rainfall rate of about 6.6 mm/hr, corresponding to about 3 dB rain attenuation.

Acknowledgments This work was supported by the National Science Council and National Space Program Office (NSPO) of the Republic of China under grants NSC88-2111-M-008-032-A10 and NSC89-NSPO-A-ECP-008-01, respectively.

REFERENCES

- Chu, Y. H., T. S. Hsu, L. H. Chen, J. K. Chao, C. H. Liu, and J. Rottger, 1990: A study of the characteristics of VHF radar echo power in the Taiwan area. *Radio Sci.*, **25**, 527-538.
- Chu, Y. H., L. P. Chian, and C. H. Liu, 1991: The investigations of the atmospheric precipitation by using Chung-Li VHF radar. *Radio Sci.*, **26**, 717-729.

- Chu, Y. H., and C. S. Lin, 1994: The severe depletion of turbulent echo power in precipitation using the Chung-Li VHF Doppler radar. *Radio Sci.*, **29**, 1311-1320.
- Chu, Y. H., T. Y. Chen, and T. H. Lin, 1997: An examination of wind-driven effect on drift of precipitation particles using Chung-Li VHF radar. *Radio Sci.*, **32**, 957-966.
- Chu, Y. H., and J. S. Song, 1998: Observations of precipitation associated with a cold front using a VHF wind profiler and a ground-based optical rain gauge. *J. Geophys. Res.*, **103**, 11,401-11,409.
- Crane, R. K., 1980: Prediction of Attenuation by Rain, Proc. IEEE Trans. Comm., COM-28, 1717.
- Harrold, T. W., 1967: Attenuation of 8.6 mm Wavelength Radiation in Rain, Proc. Inst. Elec. Eng., 114, 201.
- Hogg, D. C., Rain, 1989: Radiometry, and Radar, IEEE Trans. Geosci. Remote Sensing, **27**, 576.
- Hogg, D. C., and T. S. Chu, 1975: The Role of Rain in Satellite Communications. Proc. IEEE, **63**, 1308.
- Ippolito, Jr., L.J., 1986: Radiowave Propagation in Satellite Communication, Van Nostrand Reinhold Company, New York, NY.
- Ippolito, Jr., L. J., and T. A. Russell, 1993: Propagation Considerations for Emerging Satellite Communications Applications. Proc. IEEE, **81**, 923.
- Olsen, R. L., D. V. Rogers, and D. B. Hodge, 1978: The aR^b Relation in the Calculation of Rain Attenuation, IEEE Trans. Antenna Propagator., AP-26, 318.
- Ottersten, H., 1969: Radar backscattering from the turbulent clear atmosphere, *Radio Sci.*, **4**, 1251-1255.
- Rogers, R. R., 1979: A short course in cloud physics, 2nd edition, 235pp, Pergamon Press, New York.
- Samplak, R. A., and R. H. Turrin, 1969: Some Measurements of Attenuation by Rainfall at 18.5 GHz. *Bell Syst. Tech. J.*, **48**, 1767.
- Shih, S. P., and Y. H. Chu, 1999a: Ka band propagation experiment of experimental communication payload (ECP) on ROCSAT-1 – Preliminary results. *TAO, Supplementary Issue*, 145-164.
- Shih, S. P., and Y. H. Chu, 1999b: Estimations of precipitable water vapor content using a single 19.5 GHz ground-based radiometer, submitted to *J. Appl. Meteorol.*
- Tatarskii, V. I., 1971: The effects of the turbulent atmosphere on wave propagation, Trans. by Israel Program for Sci. Transl., Jerusalem, IPST Cat No. 5319 UDC 551.510, TSNB 0-7065-0680-4, 471pp.
- Tsuda, T., P. T. May, T. Sato, S. Kato, and S. Fukao, 1988: Simultaneous observations of reflection echoes and refractive index gradient in the troposphere and lower stratosphere. *Radio Sci.*, **23**, P.655-665.